ISSN impresa 0717-3644
ISSN online 0718-221X

Maderas. Ciencia y tecnología 2023 (25): 19, 1-14

DOI: 10.4067/s0718-221x2023000100419

COMPARING THE STRUCTURE OF SPRUCE WOOD BIODEGRADED BY *Trametes versicolor* AND *Gloeophyllum trabeum* AND FURTHER UTILIZATION OF THIS MATERIAL

***Oľga Mišíková*[1]**

https://orcid.org/0000-0003-2631-5628

***Barbora Slováčková*[1,♠]**

https://orcid.org/0000-0002-7327-6302

ABSTRACT

Development of new materials puts a great emphasis on saving production costs, energy, decreasing the amount and number of chemicals used during the manufacturing process. Bio-based materials can be ecologically produced and recycled after their lifespan, which saves the environment. The recent interest in bio-based materials led to the objective of this work. In this article, the structure of spruce wood (*Picea abies*) biodegraded by the white-rot fungus *Trametes versicolor* and brown-rot fungus *Gloeophyllum trabeum* was studied. Structure of the wood was observed macroscopically and microscopically. Classic and unusual stain combinations were used in this work. Ethanol was intentionally omitted in the process of making permanent mounts. It was done to preserve the coherence of the decayed microsections and to keep small fragments from being rinsed away. Results of the observations suggest that spruce wood decayed by these fungi could be used as an insulation material. Wood decaying fungi decrease the density of wood and increase its porosity. A low density and high porosity are important properties for insulation materials. According to the results, spruce wood decayed by *Trametes versicolor* would be more suitable to be used as an insulating material.

Keywords: Anatomy of wood, *Gloeophyllum trabeum*, light microscopy, spruce wood, *Trametes versicolor.*

INTRODUCTION

The focus in material development in the recent years has been creating materials, which are ecological, recyclable and have a low or no carbon dioxide emissions. Development of new materials and manufacturing technologies is rapidly going forward. Desired properties of a certain material can be reached by its various modifications. Modifications in material manufacturing can save energy needed for the production, number and amounts of chemical substances used and impact of the production on the environment.

Wood modifications have an abundant history. The three methods used commercially are chemical, thermal, and impregnation modification. Each of these has advantages and disadvantages when it comes to the properties of the modified wood and the complexity of the modification process (Hill 2011). Biomodification of wood with wood decaying fungi is another type of wood modification. During the early 1960s, industrially cultivated white rot fungus (*Trametes versicolor*) was used in the German Democratic Republic, mainly on beech wood for pencil or ruler production (i.e., "mykowood," Unbehaun *et al*. 2000, Mai *et al.* 2004, Schwarze and Schubert 2011).

[1]Technical University in Zvolen. Department of Wood Science. Zvolen, Slovakia.
[♠]Corresponding author: xslovackova@tuzvo.sk
Received: 27.05.2022 Accepted: 10.02.2023

Currently, fungi are widely used in multiple different areas - mycoremedation ecology, cleaning industrial sewerage water, degradation of pesticides, biosorption of heavy metals (Pavlík 2013). Natural processes that occur during fungal biodegradation of wood may be utilized for industrial purposes and have a great potential for the cellulose-producing and wood processing industries (Fackler *et al.* 2007). Using wood decay fungi for biotechnological applications in the forest products industry has been studied for several decades because the specificity of their enzymes and the mild conditions under which degradation proceeds make them potentially suitable agents for wood modification (Majcherczyk and Hüttermann 1998, Messner *et al.* 2002, Schwarze 2008).

An interesting application of a controlled use of the degradation pattern of *Physisnosporinus vitreus* is the production of mycowood with improved acoustic properties to overcome the shortages of natural wood with the superior tonal qualities desired by traditional musical instrument makers (Schwarze and Schubert 2011). Biodegradation of beech wood with *Trametes versicolor* changed its optical properties; with the amount of lignin removed an increase in the lightness and a change in the biodegraded beech wood color were observed (Solár *et al.* 2006).

The objective of this work was to compare the structure of spruce wood biodegraded by a white-rot fungus *Trametes versicolor* and a brown-rot fungus *Gloeophyllum trabeum*. Structure of the samples was observed on a macroscopic and microscopic level. Because biodegraded wood is very fragile, improving some steps in making permanent mounts process was needed. Discussion of this article explores how changes in structure of biodegraded wood affect its properties. As it was mentioned before, this change in properties can be used in the production processes or new products.

T. versicolor is known for causing both erosive and simultaneous types of decay. First, it creates cavities in S3 layers of cell walls. Cavities are created in the place of direct contact with hyphae and the gradually grow deeper and wider into the cell walls. In moderate stages of decay, certain parts of cell walls are gradually being completely digested in the direction towards the middle lamella. In advanced stages of decay, erosion channels are created (Reinprecht 1998).

Gloephyllum trabeum is a brown-rot fungus. A typical sign of brown-rot decay are cracks running across and parallel to the grain. It is a result of mechanical damage in cell walls. In brown-rot fungi decay processes, the S2 layer is the most accessible and the compound middle lamella is the least accessible to decay. Various brown-rot fungi have different abilities of degrading lignin (Reinprecht 1998).

MATERIALS AND METHODS

Spruce wood (*Picea abies* L.) samples were used in this experiment. The samples were cut from lumber obtained from a local window frames manufacturer. The obtained lumber was certified window scantlings lumber. The samples were cut and sanded to sizes of L × R × T: 8 mm × 50 mm × 50 mm, 50 mm × 8 mm × 50 mm, 50 mm × 50 mm × 8 mm. The grain was always properly aligned with the general anatomical directions. One part of the samples (48 samples) was intentionally degraded with *Trametes versicolor* (L. Lloyd), and the other part of the samples (48 samples) was intentionally degraded with *Gloeophyllum trabeum* (Pers. (Murill)). Reference samples (36 samples) were left undegraded by fungi. The mass losses of the samples were 43,8 % after degradation by *Trametes versicolor* and 20,9 % after degradation by *Gloeophyllum trabeum*.

The intentional degradation was performed in the laboratory at the Department of Wood Technology at the Technical University at Zvolen. Kolle flasks and the malt agar soil were prepared according to STN EN 113 (1998). Fungi strains used for the intentional degradation were BAM 116 for *T. versicolor* and BAM 115 for *G. trabeum* (Bundesanstalt für Materialforshung und -prüfung, Berlin, Germany). Spruce samples were submerged into re-boiled and cooled distilled water one day prior to placing the samples into prepared Kolle flasks.

Duration of the intentional degradation for *T. versicolor* was 6 months. For *G. trabeum*, the degradation time was 4 months. A shorter degradation duration for spruce samples degraded with *G. trabeum* was chosen, because samples with a longer degradation duration were too brittle to be cut into microsections. After the degradation duration passed, the samples were cleaned off visible mycelium and left to air dry at room tem-

perature. The samples were then oven dried, and they were stored in a climatic room at an air temperature 20 °C and air humidity around 50 %.

Three samples from each group (degraded by *T. versicolor*, *G. trabeum*, undegraded reference group), nine samples in total were chosen for the macroscopical and microscopical observation. From the degraded spruce sample groups, samples with a mass loss close the average mass loss of the group were chosen. The chosen samples were macroscopically observed under a Leica stereoscope. The results are shown in Figure 3e1, Figure 3e2, Figure 3e3, Figure 3g1, Figure 3g2, Figure 3g3.

After the macroscopical observation was finished, small blocks with the dimensions of 3 mm × 3 mm × 7 mm were carefully cut from the samples. A total of 9 blocks from 9 samples were used for microscopical observation. All sample blocks were embedded in epoxy resin. Embedding the decayed samples was necessary for microtome sectioning, because these samples were very fragile, and it was nearly impossible to cut the microsections. Embedding the wood blocks in epoxy resin made the fragile decayed wood stable enough for microsections cutting.

The wood samples were cut on a sledge microtome (Reichert, Wien, Austria). Thickness of the samples was approximately 15 μm - 20 μm. The microsections were put on a microscope slide and each microsection was stained with a different stain or combination of stains.

The main aim for staining microsections was to make *T. versicolor* and *G. trabeum* hyphae clearly visible in the structure of the spruce wood. Therefore, stain combinations were used to stain the spruce wood microsections. The stain combinations were made by mixing equal volumes of Toluidine, Astra Blue, Safranin and Fast Green for the TASG stain combination. For the TAS stain combination, equal volumes of Toluidine Blue, Astra Blue and Safranin were mixed. Some microsections were stained with only Toluidine or Safranin. Two more stain combinations were used in this article – the combination of Fast Green with Safranin (later referred to as GS stain combination), and Toluidine mixed with Safranin (later referred to as TS stain combination).

Using a Toluidine Blue stain gives a qualitative determination of lignin and its distribution (Herr 1992, Schwarze *et al.* 2000a, Schwarze *et al.* 2000b). Safranin stain is used for a semi-qualitative detection of lignin in cell walls. It is used as a counterstain in some staining protocols, coloring all cell nuclei red (Cartwright 1929, Jensen 1962). A combination of Safranin and Astra Blue is used to detect early stages of white rot, i.e., selective delignification. Safranin stains lignin regardless of whether cellulose is present, whereas Astra Blue stains cellulose only in the absence of lignin (Srebotnik and Messner 1994, Schwarze and Engels 1998). According to the manufacturer, Fast Green is suitable also for staining protein and starch and it is certified for use in combination with Safranin for plant cells; as a substitute for aniline blue in Gomori's one step tri-chrome procedure. Fast Green is also used as a counterstain in detecting reaction wood. Reaction wood absorbs the green stain whereas opposite wood has a red to yellow color (Kúdela and Čunderlík 2012). Uptake of dye clearly depends on both chemical and physical aspects (Hubbe *et al.* 2019).

After leaving the stain absorb in the microsections for 5 minutes, the stains or stain combinations were rinsed out with distilled water without using ethanol. Preserving most of the decayed microsection was our objective. After rinsing the microsections with only distilled water without using ethanol, they were left to air-dry. The microsections were mounted in Euparal (BioQuip Products Inc., Rancho Dominguez, United States) and covered with cover slips. The permanent microslides were placed on a board from a ferromagnetic material and magnetic weights were applied on the cover slips. The permanent microslides were left to cure at room temperature for two to three weeks.

We intentionally omitted the step of using ethanol for drying microsections. Further rinsing steps could damage the hyphae, and small fragments of the decayed wood could be rinsed away. We also wanted to omit ethanol to avoid using more chemical substances to prepare the fragile microsection. The comparison of leaving the microsections to air-dry without using ethanol and using ethanol to dry the microsection are shown in Figure 1.

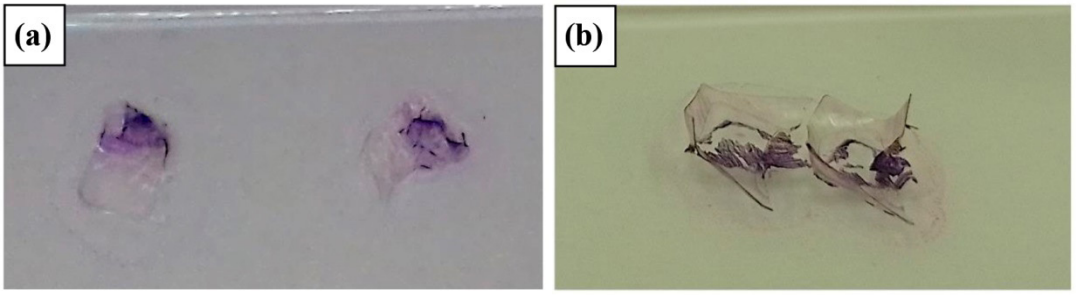

Figure 1: Difference between *Gloeophyllum trabeum* decayed spruce wood microsections rinsed with only distilled water and rinsed with using ethanol. (a) Microsections rinsed with distilled water without using ethanol and left to air-dry. (b) Microsections rinsed with distilled water and dried with 75 % and 96 % ethanol.

The microsections shown in Figure 1a were rinsed only with distilled water without using ethanol after staining and they were left to air-dry at room temperature. As the photo shows, these microsections remained stretched out on the microscope slide. Microsections shown in Figure 1b were rinsed with distilled water, subsequently dried with 75 % ethanol and then with 96 % ethanol. It is apparent, that the microsections in Figure 1b are severely damaged and incoherent in comparison to microsections in Figure 1a. The microsections in Figure 1b show also severe cupping. Such cupping makes the microsections difficult to stretch out on the microscope slide.

Wood decayed with fungi is very fragile. It is therefore better to omit ethanol to dry the microsections. Ethanol causes the microsection to dry rapidly and this damages the microsection. Rinsing the microsection only with distilled water without using ethanol and leaving it to air-dry does not cause stress to the microsection. Gradual air-drying of the decayed wood microsection makes better conditions for the finished permanent mount.

Figure 2a1, Figure 2a2, Figure 2b1, Figure 2b2, Figure 2c1, Figure 2c2, , Figure 2d1, Figure 2d2 show the comparison of rinsing microsections with distilled water without using ethanol and then leaving the microsections to air-dry, and microsections where ethanol was used to dry the microsections. Microsections in Figure 2a, Figure 2a2 and Figure 2c1, Figure 2c2 were stained with TASG stain combination. They were rinsed with distilled water without using ethanol and left to air-dry. Microsections is Figure 2b1, Figure 2b2 and Figure 2d1, Figure 2d2 were stained with TAS stain combination. These microsections were dried with 75 % and 96 % ethanol.

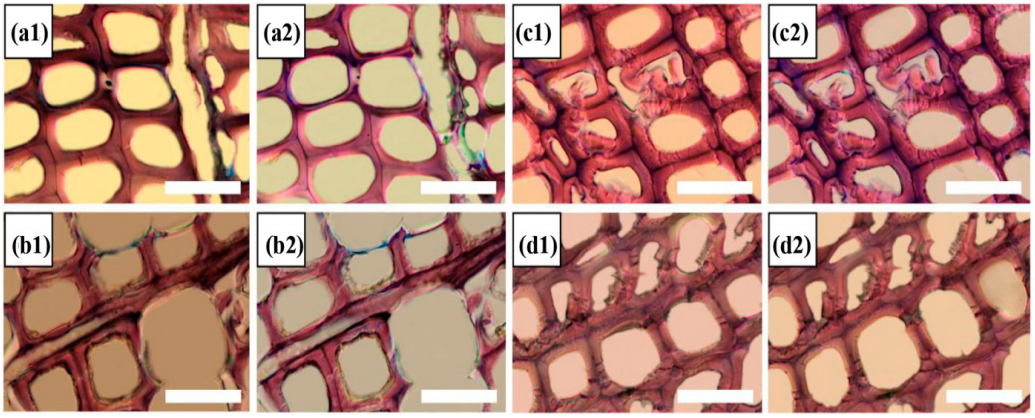

Figure 2: Cross sections of spruce wood decayed with *Trametes versicolor* (2a1 - b2) and *Gloeophyllum trabeum* (2c1 - d2). (a1, b1, c1, d1) Microsections few minutes after they were mounted with Euparal. (a2, b2, c2, d2) Microsections after 3 weeks in the finished permanent mount. The scale bar in the lower right corner of the figures is 40 µm.

The difference between leaving the microsections to air-dry without using ethanol and using ethanol to dry microsections might not be largely visible in Figure 2a1, Figure 2a2, Figure 2b1, Figure 2b2. It is visible slightly more in microsections cut from spruce wood decayed with *G. trabeum* in Figure 2c1, Figure 2c2, Figure 2d1, Figure 2d2. Cell walls in Figure 2d1, Figure 2d2 (ethanol used) appear to be broken and slowly stretching out with time in comparison to cell walls in Figure 2c1, Figure 2c2 (ethanol omitted). Omitting ethanol in the permanent mount preparation process does not have a bold difference in the final color hue of the microsection. However, it is highly beneficial for coherence of the microsections, which can be seen in Figure 1b.

RESULTS AND DISCUSSION

Results

Comparison and analysis of spruce wood decayed with *T. versicolor* and *G. trabeum* was started with a macroscopic observation of differences in the structure of decayed and reference samples. The comparison is documented in Figure 3e1, Figure 3e2, Figure 3e3, Figure 3e4, Figure 3f1, Figure 3f2, Figure 3f3, Figure 3f4, Figure 3g1, Figure 3g2, Figure 3g3, Figure 3g4. Figure 3e1, Figure 3e2, Figure 3f1, Figure 3f2, Figure 3g1 and Figure 3g2 show a cross section; Figure 3e3, Figure 3g3 and Figure 3f3 show radial sections; Figure 3e4, Figure 3f4 and Figure 3g4 show tangential sections. White arrows point at ray parenchyma, yellow arrows point at checks across the grain, white arrowheads point at mycelium and yellow arrowheads point at hyphae.

Reference spruce wood cross sections are shown in Figure 3e1 and Figure 3e2, at different magnifications.

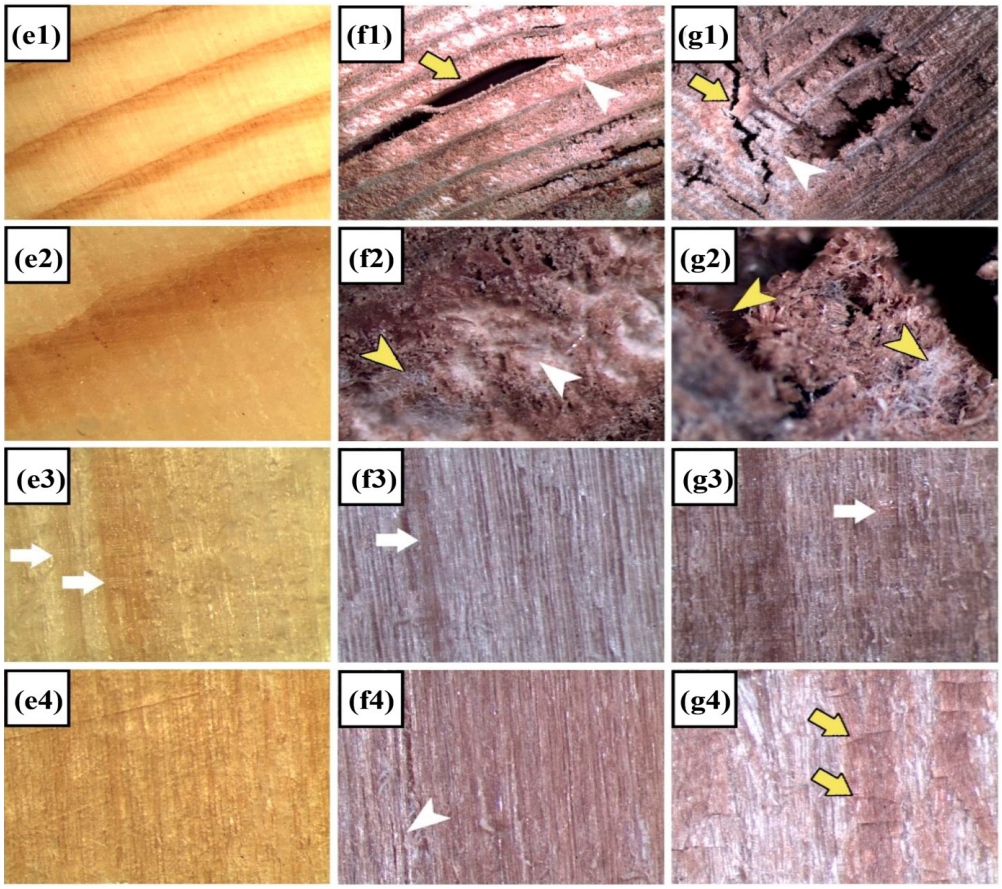

Figure 3: Macroscopical comparison of reference spruce wood (e1 - e4), spruce wood decayed by *T. versicolor* (f1 - f4) and spruce wood decayed by *G. trabeum* (g1 - g4). The magnification in Figure 3e1 is 30x, in Figure 3f1 and Figure 3g1 16x, and 60x in Figure 3e2, Figure 3e3, Figure 3e4, Figure 3f1, Figure 3f2, Figure 3f3, Figure 3f4, Figure 3g1, Figure 3g2, Figure 3g3, Figure 3g4.

The transition from earlywood to latewood is clearly visible in Figure 3e2. Both figures show earlywood and latewood. Reference spruce wood was undegraded, it has a typical pale-yellow color of earlywood and light brown color of latewood. Figure 3e3 shows a radial section of reference spruce wood. Pronounced ray parenchyma cells are visible; white arrows are pointing at them in the figure. The transition from earlywood to latewood is clearly visible in the figure. Figure 3e4 shows a tangential section of the reference spruce wood. The picture was taken at the earlywood to latewood transition; therefore, the color appears to be dark yellow to very light brown.

Figure 3f1, Figure 3f2, Figure 3f3, Figure 3f4 show spruce wood decayed with *T. versicolor*. The color change of the decayed wood is apparent. Figure 3f1 and Figure 3f2 show a cross section. A big check running along the latewood is shown in Figure 3f1. The cell walls are separated by this split. White areas visible mostly in earlywood are *T. versicolor* mycelium. Spruce wood decayed with *T. versicolor* appears to have a rough surface. In Figure 3f2, earlywood with a large area of mycelium is shown. The transition from earlywood to latewood is harder to recognize, due to the earlywood color change from pale-yellow to brown because of the decay. Earlywood cell walls around the mycelium area appear to be elevated in comparison to the cell walls covered by mycelium. Fine hyphae are also visible in this figure, they are pointed at with yellow arrowheads.

Figure 3f3 shows a radial section with exposed ray parenchyma. In comparison to the reference spruce wood radial section in Figure 3e3, the cell walls of spruce wood decayed with *T. versicolor* are more pronounced and clearly visible even at the magnification of 60 x. This is due to the activity of the fungus, thinning of cell walls made the lumina wider. In some spots, the cell walls can even be missing because they are already mostly or fully digested by the fungus. The white, shiny areas are *T. versicolor* mycelium. Figure 3f4 shows a tangential section. Like in Figure 3f3, cell walls are more pronounced because of their thinning caused by the fungus. Some cell walls in this figure are mostly or fully digested, and this appears like a check running along the grain in the left part of the figure. White, shiny areas of mycelium are visible also in tangential section.

In Figure 3g1, Figure 3g2, Figure 3g3, Figure 3g4, spruce wood decayed with *G. trabeum* is shown. Figure 3g1 shows a group of checks in a cross section. The check on the left side of the figure is cubical, which is a typical sign of brown-rot fungi decay. Compared to the check in Figure 3f1 in spruce wood decayed with *T. versicolor*, the edges of the check in Figure 3g1 in spruce wood decayed with *G. trabeum* are very rough. Supposing by the size of the checks in Figure 3g1, some cells walls might even be fully digested or collapsed. The area around the check is magnified 60 x in Figure 3g2. Hyphae grew through the tracheid lumina, the fine hyphae are visibly spreading throughout the spruce wood. The rough edges are created by detached tracheids and damaged cell walls.

Figure 3g3 shows a radial section. Ray parenchyma is visible, but not as much as in reference spruce wood (Figure 3e3) or in spruce wood decayed with *T. versicolor* (Figure 3f3). As in Figure 3f3, thinned cell walls and pronounced lumina are visible in Figure 3g3. However, the surface in Figure 3g3 appears to be wavy compared to the surface in Figure 3f3. This is because of checks running across the grain, which is another typical sign of brown-rot fungi decay. Checks running across the grain of the spruce wood are visible in the tangential section shown in Figure 3g4, yellow arrows point at the checks.

Hyphae growth and spread throughout the decayed spruce wood was analyzed on radial and tangential microsections shown in Figure 4h1, Figure 4h2, Figure 4h3, Figure 4i1, Figure 4i2, Figure 4i3. Figure 4h1 shows a latewood cross section stained with TAS stain combination. Figure 4h2 shows a tangential microsection and Figure 4h3 shows a radial microsection, both were stained with Toluidine. Figure 4i1 shows an earlywood cross section stained with TAS stain combination, Figure 4i2 shows a tangential microsection stained with Toluidine and Figure 4i3 shows a radial microsection stained with a combination of Fast Green and Safranin. Arrows point at hyphae and arrowheads point at bore holes. After staining the microsections with Toluidine, hyphae of both fungi appeared in a purple color (Figure 4h3 and Figure 4i2). Staining microsections with GS stain combination stained the hyphae green and the cell walls absorbed Safranin (Figure 4i3). The hyphae of both fungi appeared red when the microsections were stained with the TAS stain combination (Figure 4h1 and Figure 4i1).

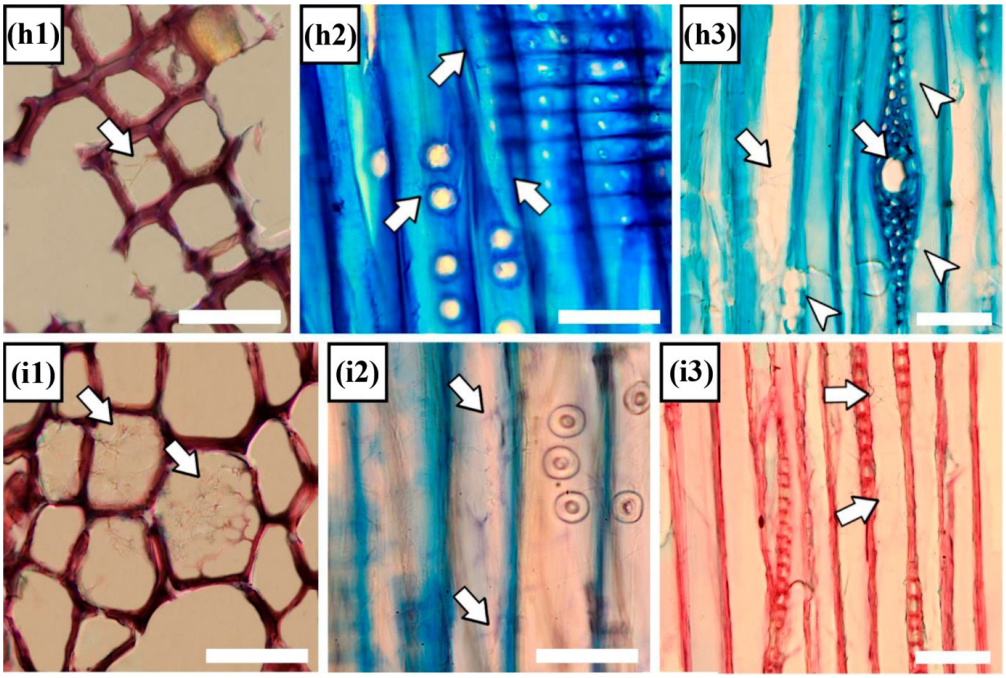

Figure 4: Hyphae in cross, tangential, and radial sections of spruce wood decayed by *T. versicolor* (h1 - h3) and *G. trabeum* (i1 - i3). The scales are denoted with a white stripe in the lower right corners of the figures, and they are 50 µm in Figure 4h1, Figure 4h2, Figure 4i1, Figure 4i2 and 75 µm in Figure 4h3 and Figure 4i3.

Hyphae of both wood decaying fungi were located mainly in lumina, which is denoted with arrows in Figures 4h1, Figure 4h2, Figure 4h3, Figure 4i1, Figure 4i2, Figure 4i3. Growth of hyphae was observed inside ray parenchyma and through resin canals (Figure 4h3, Figure 4i3). Because ray parenchyma contains nutrients, the hyphae were located mostly near ray parenchyma (Figure 4h3 and Figure 4i3). Ray parenchyma in samples decay by *T. versicolor* were often severely decomposed. This is visible v Figure 4h3, in the lower part, where an arrowhead is pointing at the ray parenchyma. Samples decayed by *G. trabeum* did not show such ray parenchyma decomposition; the ray parenchyma in these samples were undecayed (Figure 4i3). Hyphae grew also through bordered pits; this is visible in Figure 4h2. The bordered pits toruses and poruses in Figure 4h2 are almost completely digested. This was not observed in spruce wood decayed by *G. trabeum*, only a small amount of the bordered pits toruses were digested. *T. versicolor* hyphae created numerous bore holes in cell walls, which is presented in Figure 4h3. The bore holes were observed mainly on tangential sections. In this experiment, bore holes in spruce wood decayed by *G. trabeum* were not observed.

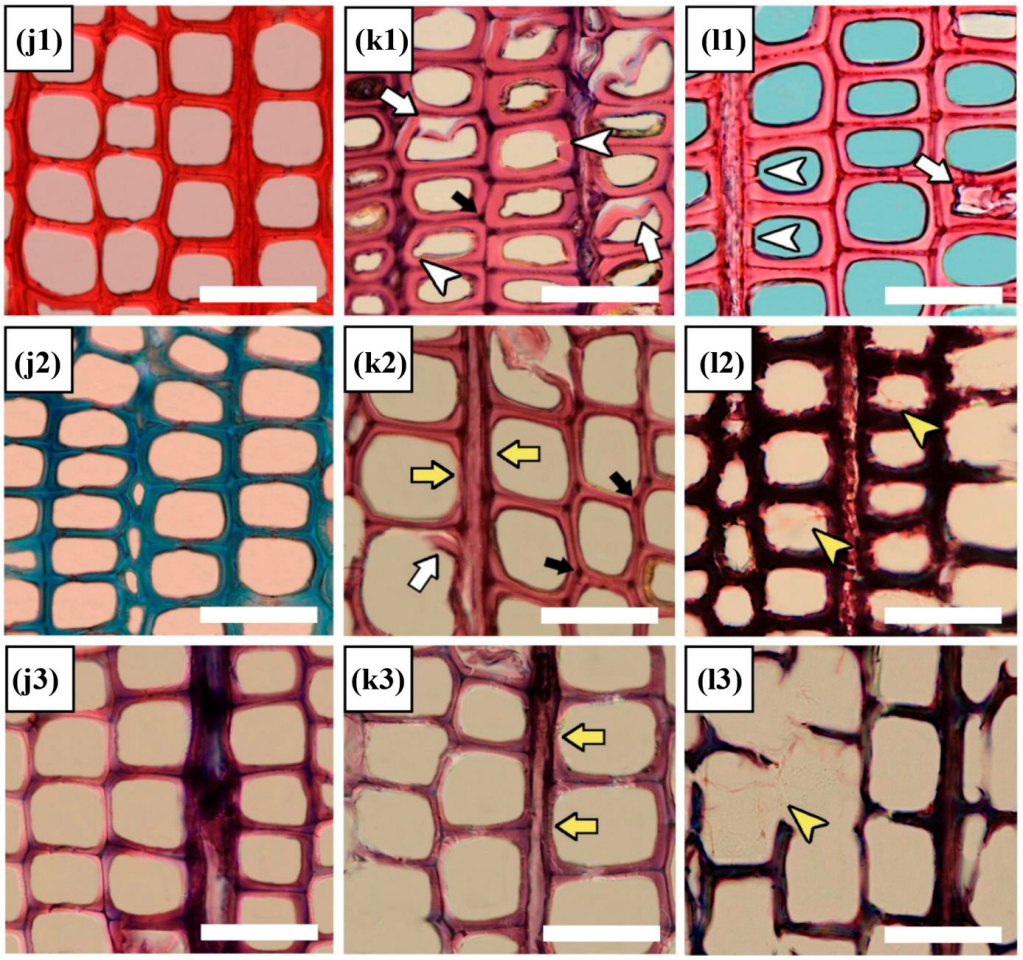

Figure 5: Comparison of latewood and earlywood spruce wood cross sections. (j1, j2, j3) Reference spruce wood. (k1, k2, k3) Spruce wood decayed by *T. versicolor*. (l1, l2, l3) Spruce wood decayed by *G. trabeum*. The scale is denoted with a white stripe in the lower right corner of the figures, and it is 50 µm.

Figure 5 shows a comparison of reference spruce wood (Figure 5j1, Figure 5j2 and Figure 5j3, the microsections were stained with Safranin, Toluidine and TASG stain combination respectively), spruce wood decayed by *T. versicolor* (Figure 5k1, Figure 5k2 and Figure 5k3, the microsections were stained with TAS, TS and TASG stain combinations respectively) and spruce wood decayed by *G. trabeum* (Figure 5l1, Figure 5l2 and Figure 5l3, microsection in Figure 5l1 was stained with the combination of Fast Green - Safranin and Figure 5l2 and Figure 5l3 were stained with the TS stain combination). White arrows in Figure 5 point at detaching and peeling cell walls, yellow arrows point at thinned cell walls, white arrowheads point at cavities, yellow arrowheads point at hyphae, small black arrows point at dark spots in the corner areas of the cell walls.

Cell walls in the reference spruce wood microsections are coherent and without any damage. The cell walls in both earlywood (Figure 5j1 and Figure 5j3) and latewood (Figure 5j2) are of the same width, without visibly thinned areas. Ray parenchyma in Figure 5j3 absorbed a blue color, whereas the cell walls are of a pale purple color.

Figure 5k1 shows numerous cavities in spruce latewood, denoted with arrowheads. The part of ray parenchyma in the upper part of the figure absorbed a blue color, the cell walls are of a pale red color. Multiple detached and peeling cell walls were observed in spruce wood decayed by *T. versicolor*. These are denoted with white arrows in Figure 5k1 and Figure 5k2. Dark spots at the joint corners of cells walls are observed in Figure 5k1 and Figure 5k2. These dark spots did not appear in reference spruce wood microsections. The dark

spots are known as the beginning point of the degradation process in the cell wall. There is visible thinning of cells walls in Figure 5k2 and Figure 5k3, marked with yellow arrows. Thinning occurred mostly around ray parenchyma area, which agrees with the locations of hyphae. The thinned parts of the cell walls attached to ray parenchyma are visibly thinner than their opposite parts connected to other earlywood tracheids. Figure 5k3 shows an erosion channel in the lower left part of the figure. The cell walls in this part were completely digested. Erosion channels were observed also in Figure 4h1.

Numerous cavities in spruce latewood decayed by *G. trabeum* are pointed out with white arrowheads in Figure 5l1. A detached cell wall is observed on the right side of the figure, denoted with a white arrowhead. Detached cell walls were not as often in spruce wood decayed by *G. trabeum* as in spruce wood decayed by *T. versicolor*. The cell walls in spruce wood decayed by *G. trabeum* were rather cracked and rough, as observed in Figure 5l2 or very thinned until middle lamella was left, as observed in Figure 5l3. Even though the cell walls in Figure 5l2 are very saturated with the stain combination, the strong saturation enhanced the outlines of the severely cracked the innermost tracheid layers. The location of hyphae and their attachment to the cell walls in Figure 5l2 agrees with the places where the severe cracking in the cell walls occurred. Figure 5l3 shows completely digested cell walls in earlywood with many hyphae present. Most of the cell walls in this figure are very thinned.

DISCUSSION

As observed by Bari *et al.* (2020), wood species had an important impact on the decay behavior of the studied white-rot fungi. Some white rot fungi have the genetic capacity to produce a wider range of enzymes and radicals, triggered by the chemical composition of cell walls and perhaps local variations in the molecular composition within the cell wall (Bari *et al*. 2020).

Stages of decay may vary throughout the sample. Even if the mass loss is high, the microsection might not contain any signs of decay or a very early stage of decay. It is therefore important to know, what stage of decay is being observed. Presence of only fine hyphae in wood should indicate an early stage of decay, while a mixture of fine and larger hyphae would suggest a moderate stage of decay (Wilcox 1993).

Bari *et al.* (2020) observed fungal decay by *T. versicolor* in Norway spruce (*Picea abies* (L.) H. Karst.). Early stages of decay, in which fungal hyphae and decay zones were detected in the innermost layer of the tracheids. *T. versicolor* showed more advanced stages of decay for latewood than earlywood (Bari *et al.* 2020). In the study by Wilcox (1993), the attack by *G. trabeum* on Douglas fir (*Pseudotsuga menziesii* (Mirb.) Franco) latewood was not observed until 7 % mass loss and occurred then only at the growth ring boundary; by 15 % mass loss, the attack extended from the transition as well. In white fir (*Abies concolor* (Gord. & Glend.) Lindl. ex Hildebr.), latewood attack by *G. trabeum* was not apparent until 25 % mass loss and was observed to come from both the boundary and transition of the growth ring.

In the presented work and results, signs of decay by *T. versicolor* were observed better and spotted easier in latewood than in earlywood. It is mainly due to the cell wall thickness; cavities especially are observed better in latewood than in earlywood. The decay by *G. trabeum* was apparent even in areas with an early stage of decay - the number of hyphae present in earlywood lumina was very high (Figure 4i3).

Postia placenta brown rot fungus hyphae were commonly seen moving cell-to-cell by penetrating bordered pits (Schilling *et al.* 2013). Erosion of the simple and bordered pits caused round or oval openings (Yilgor *et al.* 2013) in Turkish sweetgum (*Liquidambar orientalis* Mill.) heartwood decayed by *T. versicolor*.

Some fungi species penetrate through cell walls by creating bore holes. Hyphal tunnelling through cell walls is another means by which certain fungi may be able to grow through wood in which cell lumina are inaccessible (Daniel *et al.* 1992, Schwarze *et al.* 1995, Schwarze *et al.* 2004, Schwarze and Fink 1997, Schwarze and Fink 1998, Worrall *et al.* 1997). In our presented results, *T. versicolor* hyphae created numerous bore holes. The bore holes were observed mostly on tangential sections. *G. trabeum* did not create any bore holes.

Creation of bore holes by *T. versicolor* was observed in different wood species by various researchers before - in hornbeam wood (*Carpinus betulus*) (Bari *et al*. 2019), beech wood (*Fagus orientalis* Lipsky) (Bari *et al.* 2015) and Turkish sweetgum (*Liquidambar orientalis* Mill.) heartwood (Yilgor *et al.* 2013).

Only a few brown-rot fungi have been observed to grow by hyphal tunneling through cell walls (Duncan 1960, Schwarze *et al.* 2000a, Kleist and Schmitt 2001). *G. trabeum* was found to do so in the study by Schwarze and Spycher (2005) and Wilcox (1993). In the study by Wilcox (1993), *G. trabeum* hyphae created bore holes in Douglas fir (*Pseudotsuga menziesii* (Mirb.) Franco) and white fir (*Abies concolor* (Gord. & Glend.) Lindl. ex Hildebr.) wood in the earliest stages of decay. The bore holes were more readily observed in radial sections than in cross sections. The diameter of bore holes increased with progressing decay. Wilcox (1993) also observed that bore holes smaller in diameter than the penetrating hyphae were observed at the earliest stage of decay studied, while the bore holes were considerably larger than the hyphae by the time a moderate stage of decay was reached.

Some studies have reported that parenchyma cells are resistant to brown-rot decay (Worrall *et al.* 1997, Schwarze *et al.* 2000a, Schwarze *et al.* 2003). The results of the study by Yilgor *et al*. (2013) showed almost the same degree of decomposition in all types of cell walls in Turkish sweetgum (*Liquidambar orientalis* Mill.) heartwood decayed by *Tyromyces palustris*. In our study, *G. trabeum* digested ray parenchyma cells significantly less (Figure 4i3) than *T. versicolor*. Ray parenchyma cells in spruce wood decayed by *T. versicolor* were usually severely decomposed, with numerous bore holes in their vicinity (Figure 4h3).

Thinning of cell walls means that not only the fungi are capable of degrading lignin and hemicelluloses, but they can also attack cellulose polymer as well. The decomposition of S2 and S3 layers and the remainder of only a thin middle lamella are the result of the fungi using all cell wall components, which was previously reported (Wilcox 1973, Schwarze *et al.* 2004, Schmidt 2006, Schwarze 2007, Bari *et al.* 2018). Cell wall thinning was observed in both *T. versicolor* and *G. trabeum* samples in this experiment. The thinning was observed better, and it was apparent in samples decayed by *T. versicolor*. It was even possible to compare the thickness of the cell wall within one tracheid. One part of the tracheid was visibly thinner than the opposite part of the same tracheid, which is visible in Figure 5k3. Innermost parts of cell walls in samples decayed by *G. trabeum* were severely cracked and then digested until compound middle lamella was left.

In the case of brown rot degradation, cellulose has been removed leaving lignin as the cell wall component. *T. versicolor*, on the other hand, also degrades lignin so the structure after white rot degradation looks rough (Vaukner Gabrič *et al.* 2016). Roughness of both *T. versicolor* and *G. trabeum* samples is compared in Figure 3f3, Figure 3f4, Figure 3g3, Figure 3g4. The samples decayed by *T. versicolor* look more coherent and compact in comparison to samples decayed by *G. trabeum*. The structure of spruce wood decayed with *G. trabeum* appears to be sponge-like, almost fleecy, especially around areas with checks (Figure 3g2).

Presence of bore holes, thinned cell walls and erosion channels increase the porosity of decayed wood. Porosity of beech wood (*Fagus sylvatica* L.) and sessile oak heartwood (*Quercus petraea* Matt. Liebl.) decayed by *T. versicolor* was measured and calculated by Slováčková (2021b). The porosity of spruce wood was calculated in the experiment as well, but the result was published in the author´s dissertation thesis. Porosity of decayed beech wood increased by 20 % - 30 % and porosity of decayed sessile oak heartwood increased by 10 % - 13 % in comparison to healthy wood (Slováčková 2021b), and the porosity of decayed spruce wood increased by 12 % - 17 % (Slováčková 2021c). A high porosity is an important property of thermal insulations.

Because decayed wood is more porous, has wider cell lumina and there are bore holes in cell walls, the permeability of wood could be increased. However, research showed the opposite. As observed by Solár *et al.* (2006) and Slováčková and Mišíková (2021), the permeability of healthy beech wood was higher than permeability of beech wood decayed by *T. versicolor*.

A low density and high porosity of decayed spruce and beech wood were significant factors influencing the values of thermal conductivity (Slováčková 2021a). Thermal conductivity values of decayed spruce and beech wood were lower than thermal conductivity values of undecayed spruce and beech wood. Thermal conductivity measurements were performed on samples of both decayed and healthy wood conditioned at 60%±5% relative air humidity and at 20 ºC ± 2 °C air temperature. To compare the decrease in thermal conductivity values, ratios of decayed and undecayed thermal conductivities were presented: longitudinal direction in spruce 0,8; radial direction 0,64; tangential direction 0,54. The ratios for beech wood are as follows: thermal conductivities ratio of degraded and undegraded wood for longitudinal direction 0,82; for radial direction 0,61 and 0,69 for tangential direction (Slováčková 2021a).

Many of the challenges of using wood as an engineering material arise from changes in moisture content or an abundance of moisture with the wood (Glass and Zelinka 2010). Because fungi attack the cell wall components, it is expected that the fungal attack has an impact on equilibrium moisture content of the decayed

wood. Bader *et al.* (2012) observed various properties of Scots pine (*Pinus sylvestris*) sapwood decayed by *T. versicolor* and *G. trabeum*. A higher stage of degradation resulted in a lower equilibrium moisture content (EMC) and the EMC was more strongly affected by *G. trabeum* than *T. versicolor* (Bader *et al.* 2012). Chemical components of the cell wall responsible for moisture uptake are more strongly degraded by *G. trabeum* than *T. versicolor* (Bader *et al.* 2012).

CONCLUSIONS

The main objective of the presented work was to observe differences and similarities in the structure of spruce wood biodegraded by *T. versicolor* and *G. trabeum.* The samples were observed macroscopically and microscopically. Both wood decaying fungi caused thinned cell walls, numerous cavities in cell walls and a mass loss. Cutting of the decayed samples on the sledge microtome and manipulation with the microsections was difficult and it was necessary to improve the permanent mount making process. Because rinsing steps can rinse away small fragments of the fragile microsection, we tried to omit rinsing with ethanol. It was possible to rinse microsections with only distilled water and finish the permanent mount in the usual way. Wood decayed by *Trametes versicolor* could be used as insulating material. These samples had numerous bore holes in cell walls and erosion channels. The wood was very porous, had a low density, which are important properties for insulating materials. Results of this work can be applied in permanent mount preparation, material development as well as in studying effects of fungal decay on spruce wood. Biodegradation of wood is a natural process. There is a possibility of using fewer chemical substances during the production process of biodegraded wood, which can lessen the impact on the environment.

ACKNOWLEDGEMENTS

This work was supported by the Slovak Research and Development Agency (Contract No. 16-0177).

REFERENCES

Bader, T.K.; Hofstetter, K.; Alfredsen, G.; Bollmus, S. 2012. Microstructure and stiffness of Scots pine (*Pinus sylvestris* L) sapwood degraded by *Gloeophyllum trabeum* and *Trametes versicolor* - Part I: Changes in chemical, composition, density, and equilibrium moisture content. *Holzforschung* 66(2): 191-198. https://doi.org/10.1515/HF.2011.149

Bari, E.; Nazarnezhad, N.; Kazemi, S.M.; Tajick-Ghanbary, M.A.; Mohebby, B.; Schmidt, O.; Clausen, C.A. 2015. Comparison between degradation capabilities of the white rot fungi *Pleurotus ostreatus* and *Trametes versicolor* in beech wood. *International Biodeterioration & Biodegradation* 104: 231-237. https://doi.org/10.1016/j.ibiod.2015.03.033

Bari, E.; Mohebby, B.; Naji, H.R.; Oladi, R.; Yilgor, N.; Nazarnezhad, N.; Ohno, K.M.; Nicholas, D.D. 2018. Monitoring the cell wall characteristics of degraded beech wood by white-rot fungi: anatomical, chemical, and photochemical study. *Maderas. Ciencia y Tecnología* 20(1): 35-56. https://doi.org/10.4067/S0718-221X2018005001401

Bari, E.; Daryaei, M.G.; Karim, M.; Bahmani, M.; Schmidt, O.; Woodward, S.; Ghanbary, M.A.T.; Sistani, A. 2019. Decay of *Carpinus betulus* by *Trametes versicolor* - An anatomical and chemical study. *International Biodeterioration & Biodegradation* 137: 68-77. https://doi.org/10.1016/j.ibiod.2018.11.011.

Bari, E.; Daniel, G.; Yilgor, N.; Kim, J.S.; Tajick-Ghanbary, M.A.; Singh, A.P.; Ribera, J. 2020. Comparison of the Decay behavior of Two White-Rot Fungi in Relation to Wood Type and Exposure Conditions. *Microorganisms* 8(12): 1931. https://doi.org/10.3390/microorganisms8121931

Cartwright, K.ST.G. 1929. A satisfactory method of staining fungal mycelium in wood sections. *Annals of Botany* 43(2): 412-413. https://academic.oup.com/aob/article-abstract/os-43/2/412/155501?redirectedFrom=fulltext

Daniel, G.; Volc, J.; Nilsson, T. 1992. Soft-rot and multiple branching by the basidiomycete *Oudemansiella mucida*. *Mycological Research* 96(1): 49-54. https://doi.org/10.1016/S0953-7562(09)80995-7

Duncan, C.G. 1960. Wood attacking capabilities and physiology of soft-rot fungi. Report No. 2173. Forest Products Laboratory, US Department of Agriculture: Madison, WI, USA. https://ir.library.oregonstate.edu/concern/defaults/br86b7583?locale=en

Fackler, K.; Gradinger, C.; Schmutzer, M.; Tavzes, C.; Burgert, I.; Schwanninger, M.; Hinterstoisser, B.; Watanabe, T.; Messner, K. 2007. Biotechnological Wood Modification with Selective White- Rot Fungi and Its Molecular Mechanisms. *Food Technology and Biotechnology* 45(3): 269-276. https://www.ftb.com.hr/archives/72-volume-45-issue-no-3/327-biotechnological-wood-modification-with-selective-white-rot-fungi-and-its-molecular-mechanisms

Glass, S.V.; Zelinka, S.L. 2010. Chapter 4. Moisture Relations and Physical Properties of Wood. In: *Wood Handbook - Wood as an engineering material*. Robert, J.; Ross, E. E. (Eds.). General Technical Report FPL-GTR-190. U.S. Department of Agriculture, Forest service, Forest Products Laboratory: Madison WI, USA. https://www.fpl.fs.fed.us/documnts/fplgtr/fpl_gtr190.pdf

Herr, J.M. 1992. New uses for calcium chloride solution as a mounting medium. *Biotechnic & Histochemistry* 67(1): 9-13. https://doi.org/10.3109/10520299209109998.

Hill, C.A.S. 2011. Wood modification: An update. *BioResources* 6(2): 918-919. https://bioresources.cnr.ncsu.edu/resources/wood-modification-an-update/

Hubbe, M.A.; Chandra, R.P.; Dogu, D.; Van Velzen, S.T.J. 2019. Analytical Staining of Cellulosic Materials: A Review. *BioResources* 14(3): 7387-7464. https://bioresources.cnr.ncsu.edu/resources/analytical-staining-of-cellulosic-materials-a-review/

Jensen, W.A. 1962. *Botanical Histochemistry*. Freeman: San Francisco, London, United Kindgom.

Kleist, G.; Schmitt, U. 2001. Characterization of a soft-rot-like decay pattern caused by *Coniophora puteana* (Schum.) Karst. in Sapelli wood (*Entandrophragma cylindricum* Spague). *Holzforschung* 55(6): 573-578. https://doi.org/10.1515/HF.2001.093

Kúdela, J.; Čunderlík, I. 2012. *Bukové drevo – štruktúra, vlastnosti, použitie*. Technical University at Zvolen: Zvolen, Slovak Republic (Beech wood – structure, properties, and use - In Slovak)

Mai, C.; Kües, U.; Militz, H. 2004. Biotechnology in the wood industry. *Applied Microbiology and Biotechnology* 63: 477-494. https://doi.org/10.1007/s00253-003-1411-7

Majcherczyk, A.; Hüttermann, A. 1998. Bioremediation of wood treated with preservative using white-rot fungi. In: *Forest products biotechnology*. Taylor and Francis: London, United Kingdom. https://www.taylorfrancis.com/chapters/edit/10.1201/9781482272734-10/bioremediation-wood-treated-preservatives-using-white-rot-fungi-majcherczyk-h%C3%BCttermann

Messner, K.; Fackler, K.; Lamaipis, P.; Gindl, W.; Srebotnik, E.; Watanabe, T. 2002. Biotechnological wood modification. Proceedings of the International Symposium on wood-based materials. part 2. Vienna University, pp 45-49.

Pavlík, M. 2013. Možnosti využitia schopností a vlastností vybraných druhov drevokazných húb: vedecká štúdia. Technical University at Zvolen: Zvolen, Slovak Republic (Possibilities of using the abilities and properties of chosen wood decay fungi species: A scientific study - In Slovak)

Reinprecht, L. 1998. *Procesy degradácie dreva*. 2nd edition. Technical University at Zvolen: Zvolen, Slovak Republic (Processes of wood degradation – In Slovak)

Schilling, J.S.S.; Duncan, S.M.; Presley, G.N.; Filley, T.R.; Jurgens, J.A.; Blanchette, R.A. 2013. Colocalizing incipient reactions in wood degraded by the brown rot fungus *Postia placenta*. *International Biodeterioration & Biodegradation* 83: 56-62. https://doi.org/10.1016/j.ibiod.2013.04.006

Schmidt, O. 2006. *Wood and Tree Fungi: Biology, Damage, Protection, and Use*. Springer Berlin Heidelberg: Germany. https://link.springer.com/book/10.1007/3-540-32139-X

Schwarze, F.W.M.R.; Lonsdale, D.; Fink, S. 1995. Soft-rot and multiple T-branching by the basidiomycete *Inonotus hispidus* in ash and London plane. *Mycological Research* 99(7): 813-820. https://doi.org/10.1016/S0953-7562(09)80732-6

Schwarze, F.W.M.R.; Fink, S. 1997. Reaction zone penetration and prolonged persistence of xylem rays in London plane wood degraded by the basidiomycete *Inonotus hispidus*. *Mycological Research* 101(10): 1201-1214. https://doi.org/10.1017/S0953756297003808

Schwarze, F.W.M.R.; Fink, S. 1998. Host and cell type affect the mode of degradation by *Meripilus giganteus*. *New Phytologist* 139(4): 721-731. https://doi.org/10.1046/j.1469-8137.1998.00238.x

Schwarze, F.W.M.R.; Engels, J. 1998. Cavity formation and the exposure of peculiar structures in the secondary wall (S2) of tracheids and fibres by wood degrading basidiomycetes. *Holzforschung* 52(2): 117-123. https://doi.org/10.1515/hfsg.1998.52.2.117

Schwarze, F.M.W.R.; Baum, S.; Fink, S. 2000a. Dual modes of degradation by *Fistulina hepatica* in xylem cell walls of *Quercus robur*. *Mycological Research* 104(7): 846-852. https://doi.org/10.1017/S0953756299002063

Schwarze, F.M.W.R.; Baum, S.; Fink, S. 2000b. Resistance of fibre regions in wood of *Acer pseudoplatanus* degraded by *Armillaria mellea*. *Mycological Research* 104(9): 126-132. https://doi.org/10.1017/S0953756200002525

Schwarze, F.M.W.R.; Fink, S.; Deflorio, G. 2003. Resistance of parenchyma cells on wood to degradation by brown rot fungi. *Mycological Progress* 2(4): 267-274. https://link.springer.com/article/10.1007/s11557-006-0064-1

Schwarze, F.W.M.R.; Engels, J.; Matthek, C. 2004. *Fungal strategies of wood decay in trees*. 2nd ed. Springer Berlin: Heidelberg, New York, USA.

Schwarze, F.M.W.R.; Spycher, M. 2005. Resistance of thermo-hygro-mechanically densified wood to colonisation and degradation by brown-rot fungi. *Holzforschung* 59(3): 358-363. https://doi.org/10.1515/HF.2005.059

Schwarze, F.W.M.R. 2007. Wood decay under the microscope. *Fungal Biology Reviews* 21(4): 133-170. https://doi.org/10.1016/j.fbr.2007.09.001

Schwarze, F.W.M.R. 2008. Diagnosis and prognosis of the development of wood decay in urban trees. ENSPEC: Melbourne, Australia.

Schwarze, F.W.M.R.; Schubert, M. 2011. *Physisnosporinus vitreus*: a versatile white rot fungus for engineering value-added wood products. *Applied Microbiology and Biotechnology* 92: 431-440. https://doi.org/10.1007/s00253-011-3539-1

Slováčková, B. 2021a. Thermal conductivity of spruce, beech and oak heartwood degraded with *Trametes versicolor* L. Lloyd. *Acta Facultatis Xylologiae Zvolen* 63(1): 5-15. https://www.tuzvo.sk/sk/afxz-scientific-journal-12021-0

Slováčková, B. 2021b. Porosity of beech and oak heartwood degraded by *Trametes versicolor* L. Lloyd (*Fagus sylvatica*, L. and *Quercus petraea*, Matt. Liebl). 9th Hardwood Proceedings, Part II, 9(2): 98-104. http://www.hardwood.uni-sopron.hu/wp-content/uploads/2021/06/HWC2020_proceedings_final_online_II.pdf

Slováčková, B. 2021c. Nepriame úlohy z identifikácie fyzikálnych polí v hnilom dreve: Dizertačná práca. Ph. D. thesis, Technical University at Zvolen. Zvolen (Inverse problems in physical fields identification in decayed wood. Ph. D. thesis - In Slovak)

Slováčková, B.; Mišíková, O. 2021 Permeability of three wood species degraded by Trametes versicolor L. Lloyd. *Acta Facultatis Xylologiae Zvolen* 63(2): 5-15. https://df.tuzvo.sk/sites/default/files/01-02-21_0_0_0.pdf

Solár, R.; Kurjatko, S.; Mamoň, M.; Neuschlová, E.; Hudec, J. 2006. Selected chemical and physical properties of beech wood degraded by wood destroying fungi. Part 1: degradation by *Trametes versicolor*. *Wood Structure and Properties '06.* pp.381-387.

Srebotnik, E.; Messner, K. 1994. A simple method that uses differential staining and light microscopy to assess the selectivity of wood delignification by white rot fungi. *Appl Environ Microbiol* 60(4): 1383-1386. https://pubmed.ncbi.nlm.nih.gov/16349245/

STN. 1998. Wood preservatives. Test method for determining the protective effectiveness against wood destroying basiodiomycetes. Determination of the toxic values. STN EN 113. Bratislava, Slovakia.

Unbehaun, H.; Dittler, B.; Kuhne, G.; Wagenfuhr, A. 2000. Investigation into the biotechnological modification of wood and its application in the wood-based material industry. *Acta Biotechnology* 20(3-4): 305-312. https://onlinelibrary.wiley.com/doi/abs/10.1002/abio.370200311

Vaukner Gabrič, M.; Boncina, T.; Humar, M.; Pohleven, F., 2016. Laccase treatment of Norway spruce wood surface improves resistance and copper fixation of treated wood. *Drewno* 59(198): 19-33. https://doi.org/10.12841/wood.1644-3985.179.10

Wilcox, W.W. 1973. Degradation in relation to wood structure. In: *Wood deterioration and its preservation by preservative treatments*. Nicholas, D.D. (Ed.) Syracuse University Press: Syracuse, USA.

Wilcox, W.W. 1993. Comparative morphology of early stages of brown-rot wood decay. *IAWA Journal* 14(2): 127-138. https://brill.com/view/journals/iawa/14/2/article-p127_2.xml

Worrall, J.J.; Anagnost, E.; Zabel, R.A. 1997. Comparison of wood decay among diverse lignicolous fungi. *Mycologia* 89(2): 199-219. https://doi.org/10.1080/00275514.1997.12026772

Yilgor, N.; Dogu, D.; Moore, R.; Terzi, E.; Kartal, S.N. 2013. Evaluation of Fungal Deterioration in *Liquidambar orientalis* Mill. Heartwood by FT-IR and Light Miscroscopy. *BioResources* 8(2): 2805-2826. https://bioresources.cnr.ncsu.edu/resources/evaluation-of-fungal-deterioration-in-liquidambar-orientalis-mill-heartwood-by-ft-ir-and-light-microscopy/